ANNALES
UNIVERSITATIS MARIAE CURIE-SKŁODOWSKA
LUBLIN — POLONIA
VOL. LIV, 23 SECTIO D 1999

II Zakład Radiologii Lekarskiej Akademii Medycznej w Lublinie
Kierownik: prof. dr hab. Stanisław Bryc

WITOLD KRUPSKI, JANUSZ ZŁOMANIEC, STANISŁAW BRYC

The use of virtual 3D CT in diagnosing some intracranial diseases

Zastosowanie wirtualnej 3D TK w diagnostyce niektórych schorzeń śródczaszkowych

Dynamic development of computerised tomography techniques has increased their diagnostic potential. The use of thin, high resolution sections and of multiplanar reconstructions has been commonly recognised and gained considerable status in the diagnostics of many human organs.

2D CT pictures do not always provide full information about spatial configuration of complex anatomical structures under both normal and pathologic conditions (12).

3D CT techniques supplement the diagnostics with spatial pictures (4, 14, 21, 23).

The aim of the paper is presentation of own experiences in the use of 3D CT reconstructions for simulated assessment of normal and pathological intracranial structures.

MATERIAL AND METHODS

The material comprises 33 subjects of both sexes, aged 4–76 years, examined in our department, mainly because of injuries (16 patients) and other diseases according to the commonly accepted procedural algorithm (17). The equipment used was AR.T. by Siemens with 512 x 512 pixel matrix.

In 9 patients Ultravist was administered intravenously to show mutual relations of pathologic changes to adjacent vascular structures.

In 3D CT reconstructions values of –150 H.u. level were used for bone structures. For tumoral changes well enhanced by contrast medium and for vessels these values ranged from 50 to 150 H.u. (mean 100 H.u.). For visualising the ventricular system and hypodensive intracranial changes the levels used were from 0 to 35 H.u. (mean 17.5 H.u.).

The reconstructed picture was rotated in optional axes and set at selected angles to obtain optimal projections. Selected fragments of pictures were cut off along selected planes or from the front revealing the examined spaces. Possibilities of lighting the pictures from different directions were used obtaining optimal exposition of pathologic structures.

RESULTS

3D CT reconstructions revealed in full scope normal structures of the skull as well as the size, shape of bone defects connected with the frontal sinus (Fig. 1). 3D CT reconstructions showed in 1 patient the spatial shape of numerous calcifications in various projections defining their relation to the cranial vault (Fig. 2). Reconstructions cut off from above, especially in oblique projections, localised them also in relation to the base of the cranium.

In 4 cases the compound fractures of the pyramid were shown which were well visible in projections from the posterior fossa of the skull (Fig. 3). In 2 other cases a linear fissure of pyramid fracture visualised on thin high resolution sections was not visible on thin high resolution layers in 3D reconstructions, 3D technique let visualise in 2 patients a fissure running within the structures of the base of posterior cranial cavity (Fig. 4). Displacement of blow–in bone fragments of the skull cover was recognised in 3 patients. In 3 cases posttraumatic and postoperative defects were shown obtaining in projections from the inside of the skull good spatial assessment of adjacent structures (Fig. 5). In conditions after craniotomy the character of the edges of defects was reconstructed. In 2 cases of gunshot wounds the bullet trajectory was localised within the cranial cavity as well as its numerous tiny fragments (Fig. 6).

In 2 patients the use of the third dimension visualised bone damages which were not recognisable by means of other imaging techniques and had been caused by a perisellar tumour (Fig. 7).

There were also obtained spatial pictures of tumour soft tissue masses which got intensely enhanced by contrast. Such pictures were obtained in 2 cases of meningiomas one of them being localised within the cerebellopontine angle (Fig. 8).

In 1 case of a small aneurysm of the arteria cerebri anterior no diagnostically valuable spatial pictures were obtained. However, in osteoma of temporal squama virtual 3D CT revealed the morphology of its surface with the sulcus of cerebral gyri. (Fig. 10).

Pathologic masses localised above the level of the base of the cranium were visualised by superior and lateral projections as was shown in the case of the recurrence of a perisellar tumour (Fig. 9).

In 3 cases of congenital hydrocephalus spatial pictures of widened cerebral ventricles were obtained. In 1 patient porencephaly communicating with big post–inflammatory hydrocephalus was recognised (Fig. 10). 3D CT reconstructions were twice used to assess subarachnoid cysts. In 2 subjects spatial reconstructions of 25–30 H.u. level were likewise used for visualising the extent of ischaemic infarctions (Fig. 11).

DISCUSSION

3D CT reconstructions improve the imaging of spatial relations by simulating direct visualisation of the lesion. They do not replace conventional sections but supplement them in the regions of complex anatomical structures (3, 4, 14, 23). In complicated injuries accurate assessment of the morphology on sections is difficult (4).

The course of fracture fissures, both within the vault and base of the skull, is better seen on spatial reconstructions than on a single 2D CT picture. Likewise, the degree of blow–in of bone fragments is better visualised in the spatial perspective. Localisation of intracranial bone fragments as well as of foreign matter of traumatic origin is more precise in the technique under discussion. The precise observation of the course of fissures on 2D CT sections, as well known, is difficult because of complex architecture of the base of the cranium (17).

In the assessment of complex lesion to the temporal bone the value of 3D CT is unquestionable (9). Simulated 3D CT, however, enables better understanding of the topography of the lesion (1, 2, 3, 9). The temporal bone is believed to be the region especially predisposed for 3D reconstruction in the high resolution programme.

In big bone defects 3D CT is used to determine the size and shape of the bone graft (7, 9).

The revealing of the extent of erosion of cranial bone structures caused by infiltration or tumour impression and resulting from other pathologic processes is optimal in three–dimensional reconstructions. In neoplastic diseases they reveal the extent of bone destruction (8).

Soft and hard programmes were produced for three–dimensional imaging of soft tissue and bone defects. The authors used appropriate reconstruction levels for visualising different structures.

Good quality pictures were obtained in tissues of big difference of density, especially those containing calcifications. Good imaging of osteomas and hiper vascularised tumours resulted from the possibility of setting a high reconstruction level which enabled the assessment of the relation of tumour to bone structures. Sophisticated computer programmes of 3D CT reconstruction make it possible to reconstruct the base of the skull and relationship of bone structures, tumour, vessels and brain ventricles in a single imaging (Fig. 6). This is especially the case with base fronto–temporal tumours, often eliminating angiography (5). It is then essential to visualise the relationship of the tumour and vessels. CT angiography of cerebral arteries using spatial reconstructions requires the use of a spiral tomograph. Unfortunately, the authors have not obtained better visualisation of the vessels by means of 3D technique with a conventional tomography.

The reduction of the reconstruction level to 0 H.u. enables spatial imaging of cysts, cystic parts of tumours and the ventricular system, especially when it is widened. The setting of the level in our conditions at 30 H.u., however, made it possible to reconstruct extensive ischaemic areas though the 3D CT picture cannot contain more details than two dimensional sections (7).

3D pictures can be rotated in optional axes and set at selected angles the reconstructed picture during rotation being watched on the monitor screen. It is possible to cut off fragments of the spatial picture and ground lighting it from different directions. Thus, the depth dimension is revealed which is essential in the analysis of cranial bone structures since axial sections do not give the impression of spatial depth (22).

It should be added that from spatial pictures the measurements of anatomical distances and volumes can be directly obtained (8). Geometrical accuracy and optimal visualisation of lesions is difficult to reconstruct by means of other techniques.

There is emphasised the usefulness of 3D CT in the assessment of congenital multiformations cerebri, especially incomplete division of the forebrain, Crouzon–Aperta and Tracher–Collins syndrome in children, fronto–ethmoid meningocele, cranial neurofibromatosis, craniosynostosis (1, 13, 15, 16, 18).

Congenital cerebral defects are assessed by means of the soft tissue algorithm. In the fronto––nasal form of meningocele asymmetries of the vault and base of the skull were found and cranio––facial defects. 3D CT visualises aplasia and agenesis of bone structures (1, 20). The benefits of 3D CT in recognising developmental and traumatic cranio–facial abnormalities are also known (18).

The usefulness of 3D reconstructions is recognised in diagnosing, planning and neurosurgical stereoscopic treatment as well as of otolaryngologic diseases (10, 11, 19). Thorough assessment of spatial topography facilitates the choice of the optimal operative technique (12).

The disadvantages of the technique include the presence of pseudodefects when the reconstruction level has been set too high as well as the lack of reconstruction of tiny fissure–like and non–displaced fracture fissures and subtle erosive changes (2, 3).

CONCLUSIONS

1. Virtual 3D CT can be used in the assessment of various intracranial pathologies enriching assessment possibilities of 2D CT axial sections and multiplanar reconstructions.

2. Spatial 3D CT pictures supplement 2D CT axial sections and planar reconstructions but cannot be a sole, independent examination.

3. Spatial reconstructions enable showing on a single picture of complex anatomical relations visible on numerous two–dimensional sections, and observation of the rotated picture makes possible the choice of the optimal projection for performing the documentation.

4. In the pathology of bone structures of complex anatomical regions thin two–dimensional section of high resolution should be enriched by virtual pictures of computerised tomography.

REFERENCE

1. Althman N. et al.: Three–dimensional CT reformation in children, A.J.R. 146, 1261, 1986.
2. Astinet F. et al.: High Resolution CT of the Petrosa with Two and Three–dimensional Reconstructions. Advances in CT, Zurich 1990, ed. Fuchs W. A. 131.
3. Bryc S. et al.: Trójwymiarowe rekonstrukcje TK w badaniach zmian urazowych kręgosłupa. Pol. Przegl. Radiol., 62, 3, 203, 1997.
4. Davis R. et al.: Three–dimensional High–resolution volume rendering (HRVR) of computed tomography data: Application to otolaryngology and neck surgery. Laryngoscope. 101, 573, 1991.
5. Dietrich J., Fried H.: Intrakranielle dreidimensionale Computertomographie in der praoperativen Hirntumordiagnostik. Zentralbl. Neurochir., 55, 42, 1994.
6. Elolf E. et al.: Three–dimensional computed tomographic reconstructions: planning tool for surgery of skull base pathologics. Comput. Aided Surg., 3, 89, 1998.
7. Fishman E. et al.: Three–dimensional Imaging. Radiology. 181, 321, 1991.
8. Friedman M. et al.: Three–dimensional imaging for evaluation of head and neck tumors. Arch. Otolaryngol. Head, Neck Surg., 119, 601, 1993.
9. Howard J. et al.: Temporal bone: Three–dimensional CT. II. Pathologic alterations. Radiology, 177, 427, 1990.

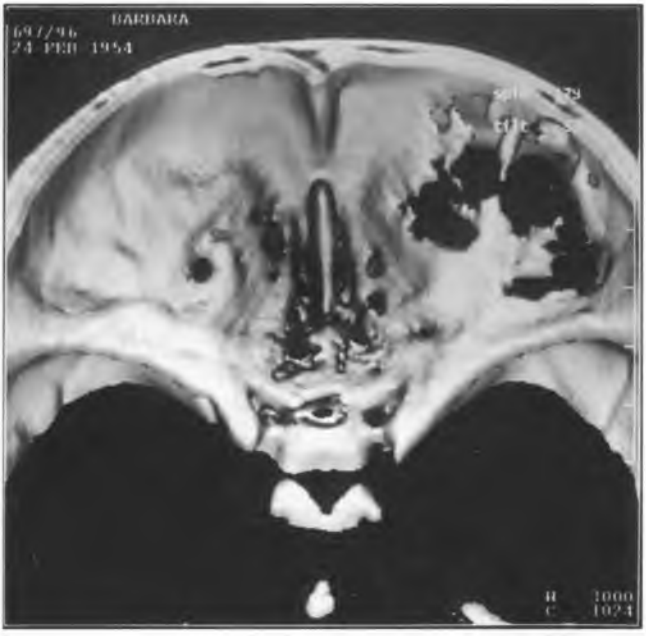
BARBARA
69/96
24 FEB 1954
R 1000
C 1024

Fig. 1

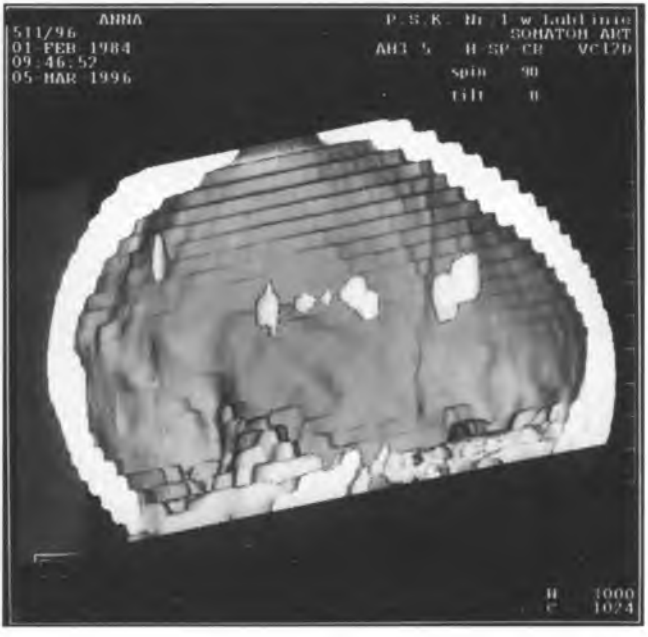
ANNA
511/96
01-FEB-1984
09:46:52
05-MAR-1996
SOMATOM AR
spin 90
tilt 0
R 1000
C 1024

Fig. 2

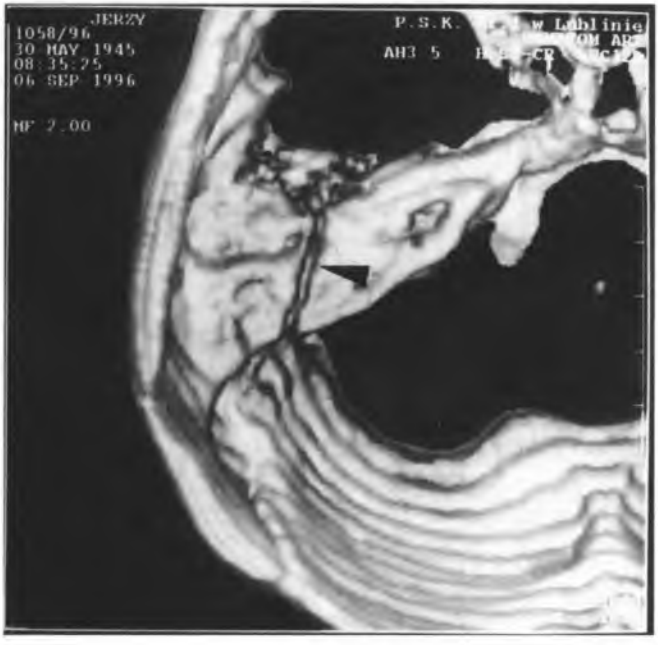
JERZY
1058/96
30 MAY 1945
08:35:25
06 SEP 1996
MF 2.00
P.S.K.
AH3 5

Fig. 3

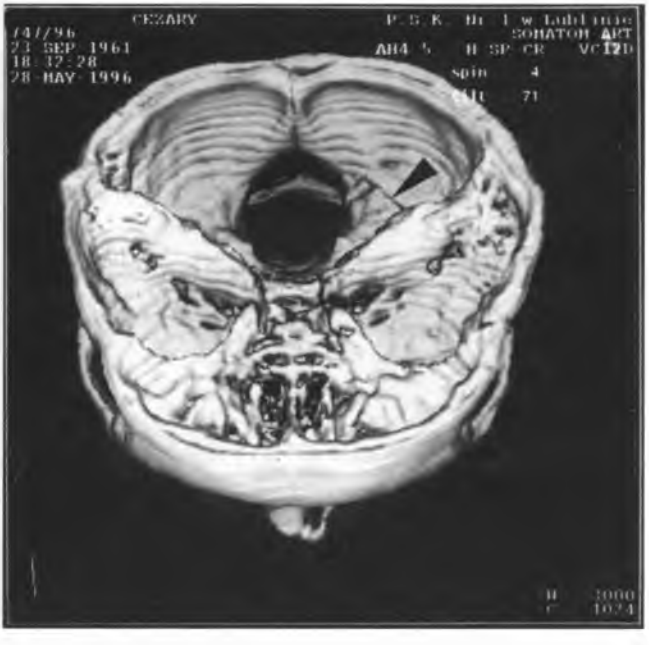
CEZARY
74//96
23 SEP 1961
18:32:28
28-MAY-1996
P.S.K.
AH4 5
spin 4
71

Fig. 4

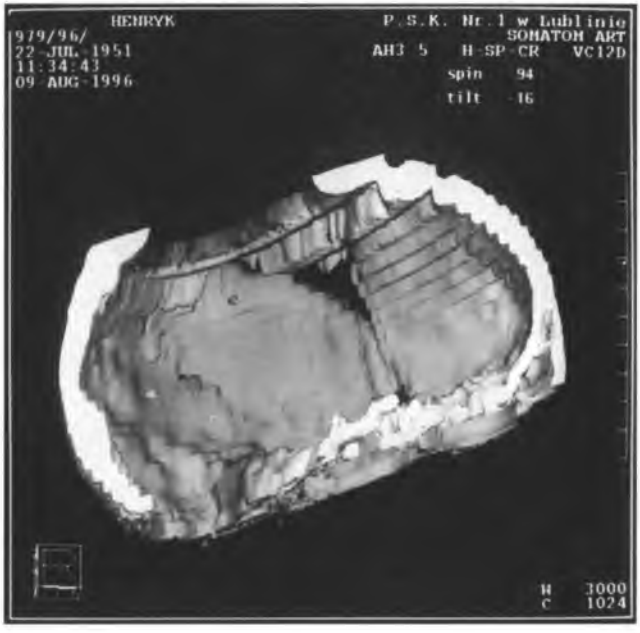
HENRYK
979/96/
22-JUL-1951
11:34:43
09-AUG-1996
P.S.K. Nr.1 w Lublinie
SOMATOM ART
AH3 5 H-SP-CR VC12D
spin 94
tilt -16
W 3000
C 1024

Fig. 5

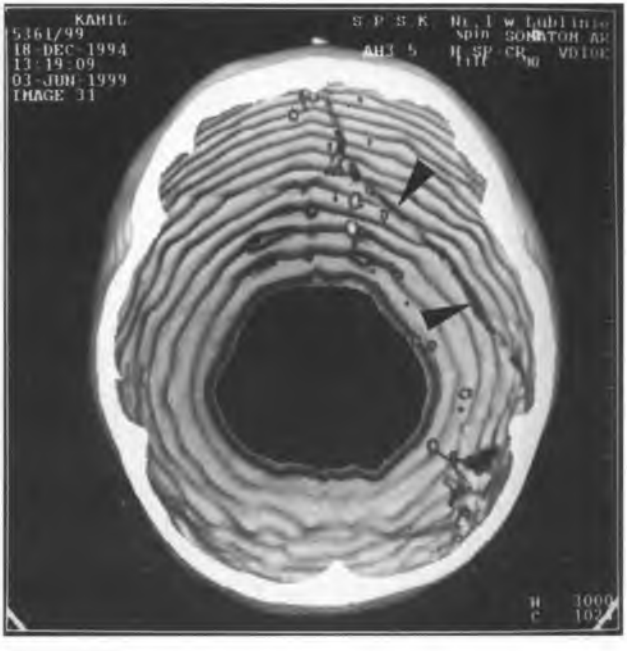
KAMIL
5361/99
18-DEC-1994
13:19:09
03-JUN-1999
IMAGE 31
S.P.S.K. Nr.1 w Lublinie
AH3 5

Fig. 6

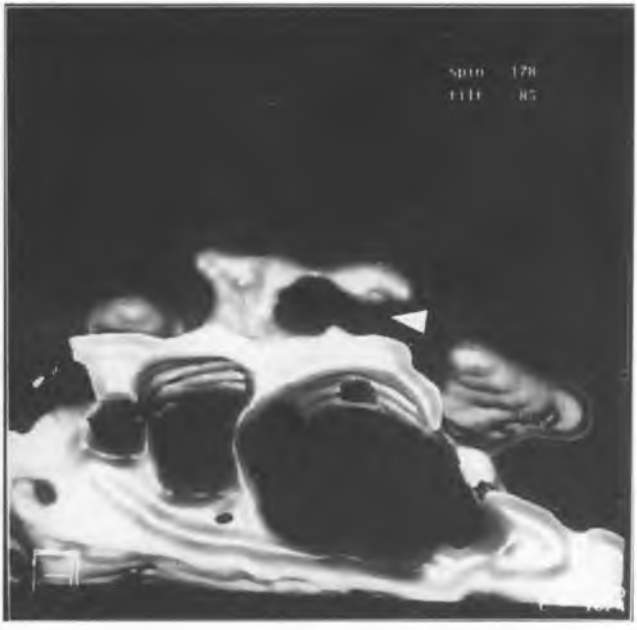

Fig. 7

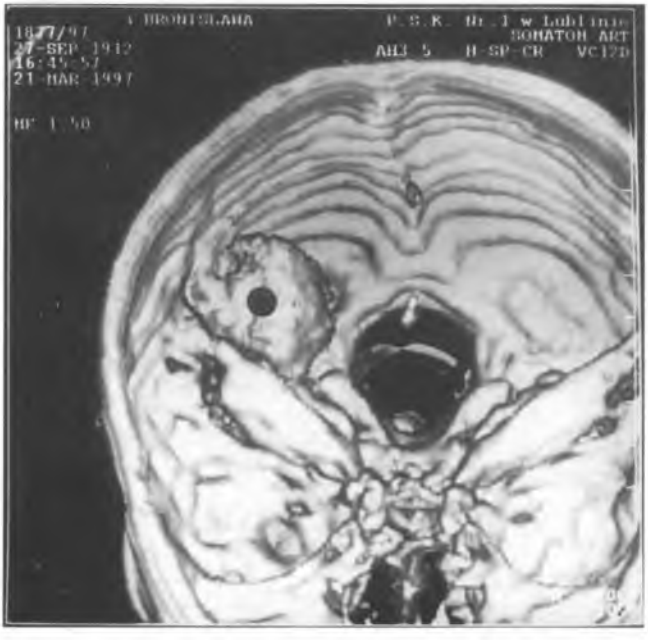
P.S.K. Nr.1 w Lublinie
SONATON ART
AH3 5 H-SP-CR VC12b
27-SEP-1912
21-MAR-1997

Fig. 8

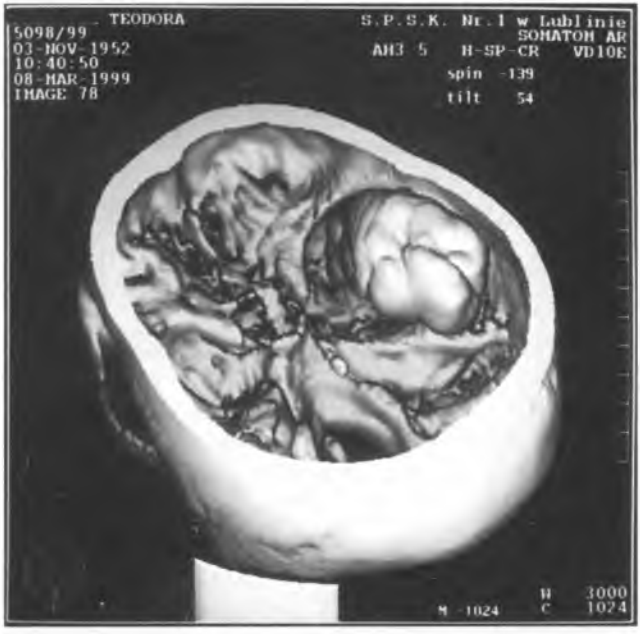
TEODORA
5098/99
03-NOV-1952
10:40:50
08-MAR-1999
IMAGE 78
S.P.S.K. Nr.1 w Lublinie
SOMATOM AR
AH3 5 H-SP-CR VD10E
spin -139
tilt 54
W 3000
C 1024
M -1024

Fig. 9

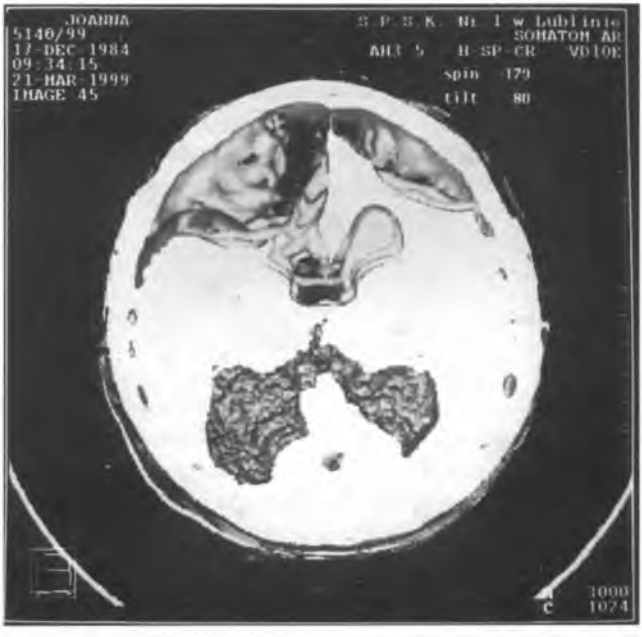
JOANNA
5140/99
17-DEC-1984
09:34:15
21-MAR-1999
IMAGE 45
S.P.S.K. Nr.1 w Lublinie
SOMATOM AR
AH3 5 H-SP-CR VD10E
spin -179
tilt 80
W 3000
C 1024

Fig. 10

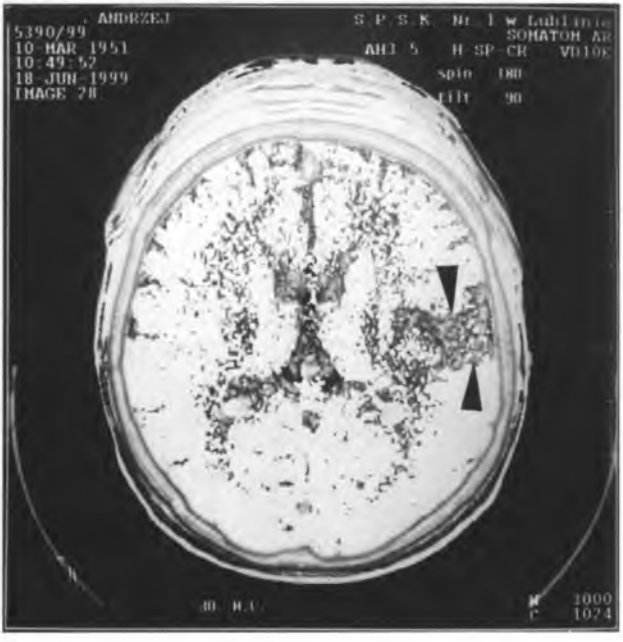
ANDRZEJ
5390/99
10 MAR 1951
10:49:52
18 JUN 1999
IMAGE 28
S.P.S.K. Nr. 1 w Lublinie
SOMATON AR
AH1 5 H SP CR VD10E
Spin 180
Tilt 90
W 1000
C 1024

Fig. 11

10. Kavanagh K.: Applications of image–directed in robotics in otolaryngologic surgery, Laryngoscope., 104, 238, 1994.
11. Klein H. et al.: Three–dimensional spiral CT for neurosurgical planning. Neuroradiology, 36, 435, 1994.
12. Kościesza A. et al.: Zastosowanie rekonstrukcji 3D w diagnostyce wybranych schorzeń OUN u dzieci. Pol. Przegl. Radiol. 62, 197, 1997.
13. Kreiborg S. et al.: Comparative three–dimensional analysis of CT scans of the calvaria and cranial base in Apert and Crouzon Syndromes. J. Craniomaxillofac. Surg., 21, 181, 1993.
14. Krupski W. et al.: 3D TK wirtualna rektosigmoidoskopia: iluzja czy rzeczywistość? Pol. Przegl. Radiol. 64, 1, 29, 1999.
15. Leboucg N. et al.: Value of 3D imaging for the study of craniofacial malformations in children. J. Neuroradial., 18, 225, 1991.
16. Leboucg N. et al.: Imagerie 3D et pathologie della base du crane chez l'enfant. Annales Radiol. (Paris)., 35, 424, 1992.
17. Łosicki M.: Możliwości opcji przestrzennej TK w wybranej patologii kostnej. Praca doktorska. Lublin 1996.
18. Ray C. Jr. et al.: Applications of three–dimensional CT imaging in head and neck pathology. Radiol. Clin. North Am. 31, 181,1993.
19. Seldom H.: Three–dimensional reconstruction of temporal bone from computed tomographic scans on a personal computer. Arch. Otolaryngol. Head Neck Surg. 117, 1158, 1991.
20. Tanaka A. et al.: Elevation of the petrous bone cased by hyperplasia of the occipital bone presenting as hemifacial spasm: diagnostic value of magnetic resonance and three–dimensional computed tomographic images in a bone anomaly. Neurosurgery. 27, 1004, 1990.
21. Tiede U. et al.: A computerized three–dimensional atlas of the human skull and brain. AJNR, 551, 1993.
22. Tomura N. et al.: Three–dimensional computed tomography in the head and neck diseases with bony abnormalites. Comput. Med. Imag. Graph., 17, 411, 1993.
23. Złomaniec J. et al.: Ocena zmian urazowych twarzoczaszki na rekonstrukcjach przestrzennych 3D TK. Ann. Univ. Marie Curie–Skłodowska, Lublin, sectio D, vol. 52, 16, 105, 1997.

Otrz.: 1999.09.10

STRESZCZENIE

W materiale 33 chorych przedstawiono możliwości diagnostyczne wirtualnych rekonstrukcji 3D TK w ocenie niektórych schorzeń śródczaszkowych. Uzyskano lepsze uwidocznienie złożonych stosunków przestrzennych podstawy czaszki, zwłaszcza w rozległych destrukcjach kostnych oraz złamaniach wielokierunkowych kości skroniowej. Uwidaczniano wzajemne stosunki guza i otaczających naczyń po iniekcji kontrastu. Lokalizację guza ułatwiało wykorzystanie wymiaru głębi przestrzennej. Rekonstrukcje 3D TK dają możliwość uwidocznienia poszczególnych części układu komorowego w dowolnym rzutowaniu. Ocena stosunków przestrzennych uszkodzenia i otoczenia ułatwia wybór optymalnej strategii postępowania, zwłaszcza w stereoskopii neurochirurgicznej.

EXPLANATIONS OF FIGURES

Fig.1. Irregular bone defect of the base of the frontal lower part of the skull caused by expansive increase of mucocoele of the right frontal sinus.

Fig.2. Intracranial calcification of postinflammatory aetiology.

Fig.3. Fracture fissure running transversely through the pyramid of the left temporal bone (arrow).

Fig.4. Fracture fissure running through the occipital bone on the left side (fracture of the base) (arrow).

Fig.5. Condition after craniotomy, projection from the inside of the skull.

Fig.6. Gunshot wound. Numerous, tiny fragments of the bullet and intracranial bone fragments, visible inlet opening and fracture fissure (arrow).

Fig.7. Raising and destruction of the posterior clinoid process on the left side by a small adenoma of hypophysis (arrow).

Fig.8. Meningioma of the right cerebellopontine angle (point).

Fig.9. Giant osteoma of temporal squama.

Fig. 10. Extensive defects of cerebral tissue within frontal lobes of porencephalic origin. Considerable widening of the ventricular system (post–inflammatory hydrocephalus).

Fig. 11. Ischaemic focus in the right cerebral hemisphere (arrows).